参 考 文 献

1 Watson BC, Noor AK. Nonlinear structural analysis on distributed-memory computers. *Computer and Structures*, 1996, 58(2): 233~247
2 Gullerud AS, Dodds Jr RH. MPI-based implementation of a PCG solver using an EBE architecture and preconditioner of implicit, 3-D finite element analysis. *Computer and Structure*, 2001, 79: 553~575
3 Petr Krysl, Zdenek Bittnar. Parallel explicit finite element solid dynamics with domain decomposition and message passing: dual partitioning scalability. *Computer and Structures*, 2001, 79: 345~360
4 邓绍忠，周树荃. 一类有限元结构分析的 EBE 计算方法. 计算结构力学及其应用， 1994, 11(3) (Deng Shaozhong, Zhou Shuquan. A class of EBE computational methods for finite element structural analysis. *Computational Structural Mechanics and Applications*, 1994, 11(3) (in Chinese))
5 李晓梅等著. 可扩展并行算法的设计与分析. 北京: 国防工业出版社， 2000 (Li Xiaomei, et al. Design & Analysis of Scalable Parallel Algorithms. Beijing: National Defence Industry Press, 2000 (in Chinese))
6 Basermann A, Reichel B, Schlthoff C. Preconditioned CG methods for sparse matrices on massively parallel machines. *Parallel Computing*, 1997, 23: 381~398

AN FEM ALGORITHM FOR PARALLEL PROCESSING COMPUTER SYSTEM

RUAN Honghe　YUAN Yong
(College of Civil Engineering, Tongji University, Shanghai 200092, China)

Abstract Traditional FEM algorithm analysis for a serial processing computer can not satisfy the demand of scientific research and engineering technology development. Parallel processing technology provides a new prospect for solving this kind of problems. Cluster parallel computer uses a very popular parallel processing method at present. Based on the features of FE Method, this paper proposes a parallel finite element algorithm, together with an Object-Oriented FEM program under multi-parallel computers with distributing memory. The calculated examples show that this algorithm improves analyzing efficiency with simple organization.

Key words parallel finite element, cluster, message passing, parallel strategy, distributed by row

左心室壁局部范围 MRI 三维有限元应变解析

王春耀　　山田宏
(新疆大学机械学院力学教研室，乌鲁木齐 830008) (日本名古屋大学工学部，日本名古屋)
刘　跃　　関岡清次
(新疆农业机械化研究所，乌鲁木齐 830091)　(日本三重大学医学部，日本津市)

摘要 利用磁共振标记技术对左心室壁进行局部三维有限元应变的分析. 在一个心动周期内，分别拍摄 24 张短轴平面图像和长轴平面图像，然后进行合成，求解出健康人左心室壁上各个位置不同时刻的位移和应变，为临床应用和定量准确地评价心功能提供重要的理论依据.

关键词 磁共振，左心室，应变

长期以来，人们应用各种不同的方法研究心肌的收缩特性，希望对心脏的动力学特性和运动规律有更加深入的了解. 随着计算机和医疗检测影像技术的发展，MRI(magnetic resonance imaging)[1] 技术不断改进，应用范围不断扩大，特别是 SPAMM(spatial modulation of magnetization)[2,3] 磁化空间调制法的出现，在收缩末期对心脏壁进行格子状的磁标记，使得磁标记格子点在整个心动周期随心脏壁同步运动，以显示心肌内部成分和收缩期室壁的运动情况，从而对标记点的移动进行追踪，使得心脏壁的变形、应变的计测、解析成为可能，为定量、客观地评价心功能提供了重要的手段.

心肌的应变状态对应着心肌重要的生理病理特性，特别是局部心室壁运动异常是冠状动脉疾病的重要特征；可以作为心肌生长、肥大和纤维化的信号 [4,5]. 因此人们试图通过量化分析左心室局部范围的运动、位移、应变等力学特性，获得一般医疗影像技术无法得到的生理病理信息 [6,7]. 本研究着眼于左心室局部变形，通过对相邻两短轴平面和长轴平面上点的追踪，依照空间位移矢量合成的方法计算空间一点或局部范围的位移、应变，为临床应用、准确地评价心功能提供重要的依据.

1 应变的计算方法

应用上述磁标记法，对志愿者的心脏左心室短轴断面

2003–03–21 收到第 1 稿， 2003–09–24 收到修改稿.

与长轴断面进行多时相连续摄像，相邻两短轴平面间距为 12 mm, 长轴平面间距为 10 mm, 如图 1 所示，断面厚度为 7mm, 一个像素 (pixel) 为 0.625 mm, 一个心动周期各获取 24 张图像，即一个心动周期分为 24 个状态，图 2 为左心室短轴 MRI 磁标记图像. 为了计算左心室局部任一点 P(追踪点) 的位移和应变 (如图 3 所示)，选两个短轴平面和两个长轴平面围成一个立方体，在立方体的交线上各选两个点，共计 8 个点，分别对 8 个点进行计算，然后利用有限元插值法计算 P 点的位移和应变. 一般情况下交线上点的位移不是图像上网格标记点，而是通过它周围的 3 个网格标记点计算得到. 设：立方体交线上点的位移为 u，第 $k-1$ 状态与 k 状态间某个标记点 (结点) 的位移用 $u^{(k)}$ 来表示，n 个状态结点的总位移可表示为

$$u=\sum_{k=1}^{n}u^{(k)} \tag{1}$$

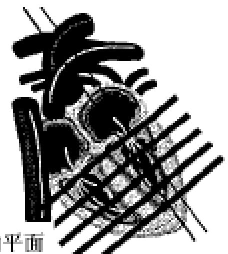

图 1 心脏左心室断面像

图 2 心脏 MRI 磁标记短轴像

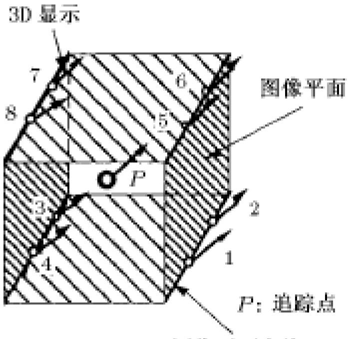

图 3 追踪点的三维有限元单元

P 点的位移为

$$u^k=\sum_{i=1}^{8}N_iu_i^k \tag{2}$$

其中 N_i 为有限元插值函数

$$\left.\begin{array}{c} N_i=\dfrac{1}{8}(1+\xi\xi_i)(1+\eta\eta_i)(1+\zeta\zeta_i) \\ (i=1,2,\cdots,8) \end{array}\right\} \tag{3}$$

式中的 N_i 是 ξ,η,ζ 的函数，求 N_i 对 x,y,z 的导数，由于涉及坐标变换的问题，变形梯度可以用局部坐标的位移分量偏导数的形式来表示

$$\begin{bmatrix} u_{1,1}^k & u_{2,1}^k & u_{3,1}^k \\ u_{1,2}^k & u_{2,2}^k & u_{3,2}^k \\ u_{1,3}^k & u_{2,3}^k & u_{3,3}^k \end{bmatrix}=\boldsymbol{J}^{-1}\begin{bmatrix} u_{1,\xi}^k & u_{2,\xi}^k & u_{3,\xi}^k \\ u_{1,\eta}^k & u_{2,\eta}^k & u_{3,\eta}^k \\ u_{1,\zeta}^k & u_{2,\zeta}^k & u_{3,\zeta}^k \end{bmatrix} \tag{4}$$

式中 $\boldsymbol{J}^{-1}$ 为雅可比矩阵的逆阵，雅可比矩阵表示为

$$\boldsymbol{J}=\begin{bmatrix} x_{1,\xi}^k & x_{2,\xi}^k & x_{3,\xi}^k \\ x_{1,\eta}^k & x_{2,\eta}^k & x_{3,\eta}^k \\ x_{1,\zeta}^k & x_{2,\zeta}^k & x_{3,\zeta}^k \end{bmatrix} \tag{5}$$

$F^{(k)}$ 为第 $k-1$ 状态与 k 状态间对应的变形梯度，变形梯度可表示为 [8]

$$\boldsymbol{F}=\boldsymbol{F}^{(n)}\ \ \boldsymbol{F}^{(n-1)}\ \cdots\ \boldsymbol{F}^{(2)}\ \ \boldsymbol{F}^{(1)} \tag{6}$$

$\boldsymbol{F}^{(k)}$ 的直角坐标形式可以用位移分量来表示

$$(\boldsymbol{F}^{(k)})_{ij}=\delta_{ij}+\frac{\partial u_i^{(k)}}{\partial x_j} \tag{7}$$

Green 应变张量可以用下式表示为

$$\boldsymbol{E}=\frac{1}{2}(\boldsymbol{F}^{\mathrm{T}}\boldsymbol{F}-\boldsymbol{I}) \tag{8}$$

或

$$E_{ij}=\frac{1}{2}(u_{i,j}+u_{j,i}+u_{m,i}u_{m,j}) \tag{9}$$

其中 $u_{i,j}$ 表示对后一项 x_j 的偏导数. 通过以上各式可以计算出各个时刻 P 点的位移和应变.

2 解析的结果

利用本方法对健康人的心脏从舒张末期到收缩末期进行计算，图 4, 图 5 为左心室的前壁 (anterior)、后壁 (posterior) 和侧壁 (lateral) 中部的位移和主应变. 图 4, 图 5 中纵坐标分别代表 P 点的位移和主应变的大小，横坐标为舒张末期到收缩末期的各个状态，u_r 为左心室径向位移，u_θ 是沿着圆周方向的位移，u_z 为心基部指向心尖的位移；E_1 是沿左心室半径方向的主应变，E_3 是沿着圆周方向的主应变. 由图可知：沿径向和轴向 (心基部指向心尖部) 的位移较大，沿圆周方向的位移较小. 图 5 表示舒张末期到收缩末期最大和最小主应变，由计算出的主应变方向余弦可知，最小主应变的方向基本上沿着圆周方向，为压应变；最大主应变的方向基本上沿着半径方向，为拉应变；故最小主应变表

示心肌收缩的程度，最大主应变表示左心室在收缩的过程中壁厚增加的程度．最大主应变的大小在 25%∼35% 之间，最小主应变的大小在 22% 左右．

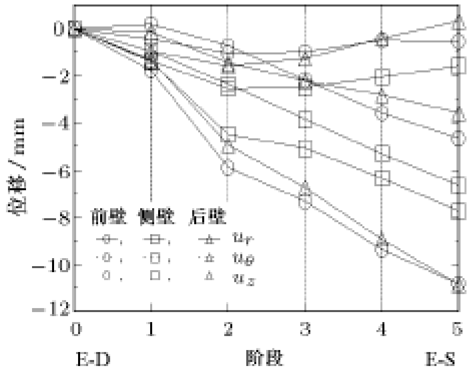

图 4　左心室局部点的位移

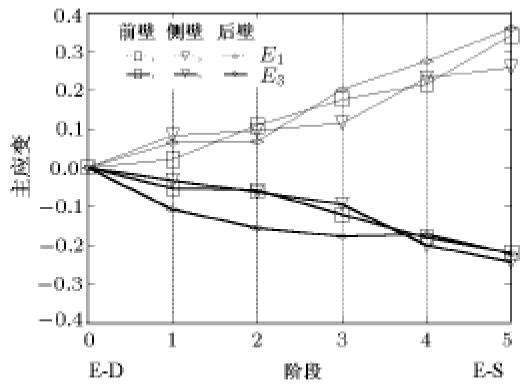

图 5　左心室局部点的主应变

参　考　文　献

1 永井辉夫编．MRI 诊断学．日本：朝仓书店，1988．278∼288 (Nagaii Kofu Ed. MRI Diagnostics. Asakura Syoten, 1988. 278∼288 (in Japanese))

2 Young AA. Two-dimensional left ventricular deformation during systole using magnetic resonance imaging with spatial modulation of magnetization. *Circulation*, 1994, 89(2): 740∼751

3 李坤成主编．心血管磁共振成像诊断学．北京：人民卫生出版社，1997．10∼12 (Li Kuncheng Ed. Magnetic Resonance Imaging Diagnostics of Heart and Great Vessels. Beijing: People's Medical Publishing House, 1997. 10∼12 (in Chinese))

4 Huisman an RM,Sipkema P,Westerhof N, et al.Comparison of models used to calculate left ventricular wall force. *Med Biol Eng Comput*, 1980, 18: 133∼144

5 王春耀，田中英一等．应用 MRI 对心脏进行平面有限元应变解析．医用生物力学，2001, 16(2): 76∼79(Wang Chunyao, Tanaka Eiichi, et al. Strain analysis of the heart with mr image based on two-dimensional method of finite element. *Journal Medical Biomechanics*, 2001, 16(2): 76∼79 (in Chinese))

6 Park J, Metaxas D, Axel L. Analysis of left ventricular wall motion based on volumetric defomabal model and MRI-SPAMM. *Medical Image Analysis*, 1996, 1(1): 53∼71

7 Moore CC, Chrios H. Three-dimensional systolic strain patterns in the normal human left ventricular: characterization with tagged MR imaging. *Radiology*, 2000, 214: 453∼466

8 Ted Belytshko, Wing Kam Liu, Brian Moran. 连续体和结构的非线性有限元. 庄茁译. 北京: 清华大学出版社, 2002. 79∼86 (Ted Belytshko, Wing Kam Liu, Brian Moran. Nonlinear Finite Elements for Continua and Structures. Zhuang Zhuo Trans. Beijing: Tsinghua University Press, 2002. 79∼86 (in Chinese))

STRAIN ANALYSES OF LEFT VENTRICLE WALL WITH THREE-DIMENSIONAL MR IMAGES BASED ON FINITE ELEMENT METHOD

WANG Chunyao* HIROSHI Yamada† LIU Yue** KIYOTSUGU Sekioka††

*(College of Mechanical Engineering, Xinjiang University Urumqi, Xinjiang 830008, China)

†(Department of Mechanical Engineering, Nagoya University, Nagoya Japan)

**(Institute of Agricultural Machinery, Xinjiang Academy of Agricultural Science, Urumqi 830091, China)

††(Department of Medicine, Mie University, Tsu Japan)

Abstract This paper proposes a three-dimensional analysis method in local regions of the left ventricle by using tagged MR imaging. The imaging slices are taken in long axis and short axis of LV wall. At least two parallel slices are prepared in each axis. The material points of interest are traced between different phases of beating heart. Two points are chosen on each intersection line of image slices which surround the trace point. Three-dimensional displacements of a point on an intersection line are derived from the two-dimensional displacements on the two perpendicular slices. By use of the interpolation function of a hexahedral element in FEM, the displacement and deformation gradients are derived from the displacements of eight nodes. Displacements of points at systole with respect to diastole can be calculated as a sum of each displacement between each phase of beating. Green's strain is also obtained by using a product of deformation gradient between each phase. The proposed method has an advantage of reducing the time of calculation by not tracing all nodal points of the finite elements in the LV wall.

Key words magnetic resonance, left ventricle, strain